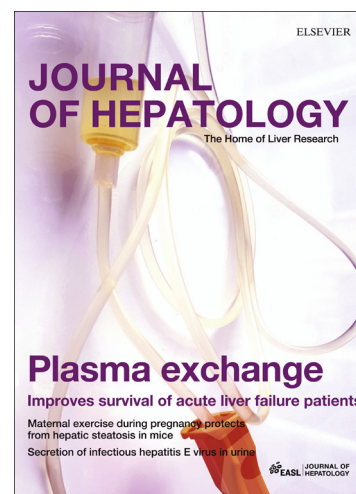


Accepted Manuscript

Malnutrition-associated liver steatosis and ATP depletion is caused by peroxisomal and mitochondrial dysfunction

Tim van Zutphen, Jolita Ciapaite, Vincent W. Bloks, Cameron Ackereley, Albert Gerding, Angelika Jurdzinski, Roberta Allgayer de Moraes, Ling Zhang, Justina C. Wolters, Rainer Bischoff, Ronald J. Wanders, Sander M. Houten, Dana Bronte-Tinkew, Tatiana Shatseva, Gary F. Lewis, Albert K. Groen, Dirk-Jan Reijngoud, Barbara M. Bakker, Johan W. Jonker, Peter K. Kim, Robert H.J. Bandsma



PII: S0168-8278(16)30263-X
DOI: <http://dx.doi.org/10.1016/j.jhep.2016.05.046>
Reference: JHEPAT 6147

To appear in: *Journal of Hepatology*

Received Date: 24 November 2015
Revised Date: 15 April 2016
Accepted Date: 30 May 2016

Please cite this article as: van Zutphen, T., Ciapaite, J., Bloks, V.W., Ackereley, C., Gerding, A., Jurdzinski, A., Allgayer de Moraes, R., Zhang, L., Wolters, J.C., Bischoff, R., Wanders, R.J., Houten, S.M., Bronte-Tinkew, D., Shatseva, T., Lewis, G.F., Groen, A.K., Reijngoud, D.-J., Bakker, B.M., Jonker, J.W., Kim, P.K., Bandsma, R.H.J., Malnutrition-associated liver steatosis and ATP depletion is caused by peroxisomal and mitochondrial dysfunction, *Journal of Hepatology* (2016), doi: <http://dx.doi.org/10.1016/j.jhep.2016.05.046>

This is a PDF file of an unedited manuscript that has been accepted for publication. As a service to our customers we are providing this early version of the manuscript. The manuscript will undergo copyediting, typesetting, and review of the resulting proof before it is published in its final form. Please note that during the production process errors may be discovered which could affect the content, and all legal disclaimers that apply to the journal pertain.

Malnutrition-associated liver steatosis and ATP depletion is caused by peroxisomal and mitochondrial dysfunction

Tim van Zutphen^{1,†}, Jolita Ciapaite^{1,2,†}, Vincent W. Bloks¹, Cameron Ackereley³, Albert Gerding¹, Angelika Jurdzinski¹, Roberta Allgayer de Moraes¹, Ling Zhang⁴, Justina C. Wolters^{2,5}, Rainer Bischoff^{2,5}, Ronald J. Wanders⁶, Sander M. Houten^{6,#}, Dana Bronte-Tinkew⁷, Tatiana Shatseva⁷, Gary F. Lewis⁸, Albert K. Groen¹, Dirk-Jan Reijngoud¹, Barbara M. Bakker^{1,2}, Johan W. Jonker¹, Peter K. Kim^{7,10 *} and Robert H.J. Bandsma^{1,4,9,11*}

¹ Department of Pediatrics, Center for Liver, Digestive and Metabolic Diseases, University of Groningen, University Medical Center Groningen, Groningen, The Netherlands

² Systems Biology Centre for Energy Metabolism and Ageing, University of Groningen, University Medical Centre Groningen, Groningen, The Netherlands

³ Department of Paediatric Laboratory Medicine, The Hospital for Sick Children, Toronto, Canada

⁴ Physiology and Experimental Medicine Program, Research Institute, The Hospital, for Sick Children, Toronto, Canada

⁵ Department of Pharmacy, Analytical Biochemistry, University of Groningen, Groningen, The Netherlands

⁶ Laboratory Genetic Metabolic Diseases, Departments of Pediatrics and Clinical Chemistry, Academic Medical Center, Amsterdam, The Netherlands

⁷ Program in Cell Biology, Hospital for Sick Children, Toronto, Canada

⁸ The Division of Endocrinology and Metabolism, Department of Medicine and the Banting and Best Diabetes Centre, University of Toronto, Toronto, Canada

⁹ Division of Gastroenterology, Hepatology and Nutrition, The Hospital for Sick Children, Toronto, Canada

¹⁰ Department of Biochemistry, University of Toronto, Toronto, Canada

¹¹ Centre for Global Child Health, The Hospital for Sick Children, Toronto, Canada

[†] These authors contributed equally to this work.

* These authors share co-senior authorship.

[#]**Current address:** Department of Genetics and Genomic Sciences, Icahn Institute for Genomics and Multiscale Biology, Icahn School of Medicine at Mount Sinai, 1425 Madison Avenue, NY 10029 New York, USA

Contact information: Robert Bandsma, Physiology and Experimental Medicine Program, The Hospital, for Sick Children, Peter Gilgan Centre for Research and Learning, 686 Bay Street, Toronto, ON M5G 0A4, Canada. E-mail: robert.bandsma@sickkids.ca, Phone: 14168137654 ext 9057; FAX: 14168134972

Peter Kim, Program in Cell Biology, Hospital for Sick Children, Peter Gilgan Centre for Research and Learning, 686 Bay Street, Toronto, ON M5G 0A4, Canada. E-mail: pkim@sickkids.ca, Phone: 14168135983; FAX: 14168135028

List of abbreviations: VLCFA, very long-chain fatty acids; FAO, fatty acid β -oxidation; TCA, tricarboxylic acid; LPD, low protein diet; QconCAT, concatamers; TG, triglycerides; ALT, alanine-aminotransferase; TBARS, thiobarbituric acid reactive substances; EM, electron microscopy; PMP70, peroxisomal membrane protein 70; DHCA, dihydroxycholestanoic acid; THCA, trihydroxycholestanoic acid; Hsp60, mitochondrial heat shock protein 60; Mfn2, mitofusin-2; PM, pyruvate plus malate; PCM, palmitoyl-CoA plus L-carnitine plus malate; SPM, succinate plus pyruvate plus malate; OXPHOS, oxidative phosphorylation; FA, fatty acid; AMPK α , AMP-activated protein kinase α subunit; Cpt, carnitine palmitoyltransferase; Acadm, medium-chain specific acyl-CoA dehydrogenase; Hadh, medium and short-chain L-3-hydroxyacyl-coenzyme A dehydrogenase; PPAR α , peroxisome proliferator-activated receptor alpha; UCP, uncoupling protein;

Keywords: malnutrition, kwashiorkor, marasmus, metabolism, hepatic steatosis, peroxisomes, mitochondria, targeted quantitative proteomics.

Conflict of interest: The authors declare that there are no conflicts of interest.

Financial Support: Robert Bandsma was supported by a North American Society for Pediatric Gastroenterology and Nutrition Foundation /Nestlé Nutrition Research Young Investigator Development Award.

Author contributions: T.Z., J.C, V.W. B., C.A., A.J., A.G., R.A.M., L.Z., D.B.T., T.S., J.C.W., R.P.B., R.W. and S.M.H. performed experiments and analyzed the data. G.F.L., A.K.G., D.J.R., J.W.J. contributed to data interpretation. T.Z., J.C, B.M.B, D.J.R., P.K.K. and R.H.J.B wrote the paper. All authors commented on the manuscript before submission.

Abstract

Background & Aims: Severe malnutrition in young children is associated with signs of hepatic dysfunction such as steatosis and hypoalbuminemia, but its etiology is unknown. Peroxisomes and mitochondria play key roles in various hepatic metabolic functions including lipid metabolism and energy production. To investigate the involvement of these organelles in the mechanisms underlying malnutrition-induced hepatic dysfunction we developed a rat model of malnutrition.

Methods: Weanling rats were placed on a low protein or control diet (5% or 20% of calories from protein, respectively) for four weeks. Peroxisomal and mitochondrial structural features were characterized using immunofluorescence and electron microscopy. Mitochondrial function was assessed using high-resolution respirometry. A novel targeted quantitative proteomics method was applied to analyze 47 mitochondrial proteins involved in oxidative phosphorylation, tricarboxylic acid cycle and fatty acid β -oxidation pathways.

Results: Low protein diet-fed rats developed hypoalbuminemia and hepatic steatosis, consistent with the human phenotype. Hepatic peroxisome content was decreased and metabolomic analysis indicated peroxisomal dysfunction. This was followed by changes in mitochondrial ultrastructure and increased mitochondrial content. Mitochondrial function was impaired due to multiple defects affecting respiratory chain complex I and IV, pyruvate uptake and several β -oxidation enzymes, leading to strongly reduced hepatic ATP levels. Fenofibrate supplementation restored hepatic peroxisome abundance and increased mitochondrial β -oxidation capacity, resulting in reduced steatosis and normalization of ATP and plasma albumin levels.

Conclusions: Malnutrition leads to severe impairments in hepatic peroxisomal and mitochondrial function, and hepatic metabolic dysfunction. We discuss the potential future implications of our findings for the clinical management of malnourished children.

Electronic word count: 251 words

ACCEPTED MANUSCRIPT

Introduction

Malnutrition still contributes to 45% of all global childhood deaths below the age of 5 years [1]. Despite great achievements in improved management of severely malnourished children, for example through development of a World Health Organization Guideline in 1999 [2], the condition remains difficult to treat and in hospital fatality rates can be more than 30% [3, 4]. In fact, it is estimated that more than a half of a million children die each year from severe malnutrition [1].

Severe malnutrition is defined by wasting but can also present with more complex phenotypical characteristics, including edema, hair discoloration, and hepatomegaly. Although a deficiency of dietary protein and calories underlie the development of severe malnutrition [5], the metabolic disturbances at the cellular level remain an enigma. Children hospitalized for severe malnutrition are initially presented with profound electrolyte disturbances, increased oxidative stress, hepatic steatosis and decreased albumin synthesis (hypoalbuminemia) [6, 7]. In addition, a recent study found an altered gut microbiome in children with severe malnutrition, further underscoring the complexity of this disease state [8].

Peroxisomes and mitochondria play key roles in various hepatic metabolic functions including lipid metabolism and energy production, and dysfunction in these organelles are linked to various disorders affecting liver, e.g. Zellweger syndrome and non-alcoholic fatty liver disease [9]. Peroxisomes are single membrane bound organelles that are important for bile acid synthesis, β -oxidation of very long-chain fatty acids (VLCFA) and cellular redox homeostasis [10], as well as the maintenance of normal mitochondrial function [11]. In turn, mitochondria are essential for aerobic ATP production, fatty acid β -oxidation (FAO) (acyl-chain length of $\leq C20$), ketogenesis and gluconeogenesis from pyruvate and tricarboxylic acid (TCA) cycle

intermediates. Defect in these two organelles have been shown to cause various degrees of liver dysfunction resulting in clinical phenotypes similar to those observed in severely malnourished individuals, e.g. increased oxidative stress and hepatic steatosis [12, 13]. Furthermore, we recently provided some evidence for a relative decrease in hepatic mitochondrial function in severely malnourished children with signs of metabolic maladaptation [14].

To study the physiological and cellular changes that drive hepatic pathogenesis in malnutrition we placed weanling rats on a low protein diet (LPD) for four weeks. Using this animal model we showed that a LPD led to early loss of hepatic peroxisomes followed by mitochondrial dysfunction with severe metabolic disturbances and energy depletion. Induction of peroxisomal biogenesis and boosting of mitochondrial FAO by fenofibrate treatment resulted in a profound amelioration of the metabolic phenotype, including normalization of serum albumin levels and restored hepatic energy status.

Materials and methods

Animals

Pregnant Wistar rats (Harlan Laboratories, Venray, The Netherlands) were housed in a temperature-controlled environment (21 °C) and 12hr, 12hr light:dark cycle with *ad libitum* access to regular chow and water. The offspring were kept with the mother until day 21 when male animals were placed on either a low protein diet (5% of calories from protein) or control diet (20% of calories from protein, as described in Table S1) (Harlan, Madison, WI, USA). Animals were kept on the diet for 1 or 4 weeks as indicated. In a different set of experiments, the offspring were weaned to a 5% protein and after 2 weeks, half of the rats received the 5% protein diet supplemented with 0.1 % (wt/wt) fenofibrate for another 2 weeks. The animal treatment conformed to the guidelines of The Institutional Animal Care and Use Committee of the University of Groningen and was in accordance with EC Directive 86/609/EEC for animal experiments.

Biochemical analyses

Plasma and hepatic metabolite analysis, enzyme activity assays and western blot analysis were carried out as detailed in the supplementary materials.

Histology & Microscopy

Livers were immediately fixed after harvesting as detailed in the supplementary materials followed by histological and ultrastructural analyses.

Isolation of liver mitochondria and high-resolution respirometry

Liver mitochondria were isolated by differential centrifugation and oxygen consumption rates were measured at 37 °C using a two-channel high-resolution Oroboros oxygraph-2 k (Oroboros, Innsbruck, Austria) as described in detail in supplementary materials.

Targeted quantitative mitochondrial proteomics

Selected 47 mitochondrial proteins involved in substrate transport, FAO and TCA cycle were quantified in isolated mitochondria using isotopically labeled standards (¹³C-labeled lysines and arginines), derived from synthetic protein concatemers (QconCAT) (PolyQuant GmbH, Bad Abbach, Germany) as described in supplementary materials.

Transcriptomics

RNA expression profiling was performed using Affymetrix Gene chip Rat Gene 1.1 ST arrays according to standard Affymetrix protocols and data were deposited to Gene Expression Omnibus (NCBI, accession number GSE63096).

Statistical analysis

All values are reported as means ± S.D. Depending on the type of experiment, Student t-test or ANOVA was used for statistical evaluation of data as described in detail in supplementary materials. All analyses were performed with IBM SPSS Statistics 22.0 (SPSS Inc., Chicago, IL, USA). Differences were considered significant at $p < 0.05$.

Results

LPD leads to severe growth retardation and hepatic steatosis

We first aimed to determine the general phenotypic effects of a LPD diet. Fig. 1 shows basic animal characteristics after 4 weeks of LPD or control diet (5% and 20% of calories from protein, respectively). We aimed to keep the total caloric density and fat content equal between the diets. The LPD-fed rats had a stunted phenotype exemplified by a lower body weight and body length. Albeit in absolute terms LPD-fed animals consumed less chow, they consumed more chow per unit body weight over time (Fig. 1A,B). However, body weight-normalized protein intake was still nearly two-fold lower at the end of the experiment, indicating that impaired growth was specifically due to lower protein intake.

As expected, plasma concentrations of essential amino acids (except histidine) were significantly lower in the LPD-fed animals (Table S3). Rao *et al.*, also noted an increase in histidine in an animal model of malnutrition and other work has also shown that histidine levels are not decreased during severe malnutrition in children [15]. The etiology is unclear, but staple foods like corn contain significant amounts of histidine and might play a role in the clinical observations. The concentrations of most non-essential amino acids were not affected or in some cases even increased (serine) compared to the controls (Table S3), suggesting metabolic compensation. The limitation of amino acids is expected to reduce protein synthesis thereby sparing amino acids that are relatively abundant in the diet. Plasma triglyceride (TG) and albumin concentrations were decreased, while alanine-aminotransferase (ALT) levels were elevated in LPD-fed animals (Fig. 1C). Lactate concentrations were comparable in both groups under fed and fasted conditions, while β -hydroxybutyrate concentrations were similar under fed conditions, but were higher in LPD group under fasting conditions (Fig. 1C), with similar insulin

concentrations (data not shown), possibly indicating a reduction in TCA cycle activity. Fasting glucose levels were lower in LPD-fed animals suggesting impaired hepatic glucose production (Fig. 1C).

The absolute liver weights were lower in LPD-fed group, while body weight-normalized liver weights were comparable (Figure 1D). The livers of LPD-fed animals were pale in color (Fig. S1A), presumably due to increased TG content, which was indeed higher compared to the controls already after one week of LPD and in line with haematoxylin and eosin staining, showing steatosis (Fig. 1D, Fig S1B). The steatosis was mainly located periportally (zone 1) and in zone 2, while the perivenous area (zone 3) was not affected. Ultrastructural electron microscopy (EM) analyses corroborated these findings (Fig. S2). Glycogen content was similar between groups (Fig. 1D, S1C). The content of thiobarbituric acid reactive substances (TBARS) was increased in livers of LPD-fed animals, suggesting increased oxidative stress (Fig. 1D).

LPD leads to diminished hepatic peroxisome content and impaired peroxisomal function

A possible cause of hepatic steatosis is the loss or dysfunction of the organelles involved in lipid catabolism. In mammalian cells, FAO occurs in both mitochondria and peroxisomes. EM revealed a near absence of peroxisomes in the periportal area of livers of LPD-fed animals compared to controls (Fig. 2A,C). Decreased immunofluorescence staining of peroxisomal membrane protein PEX14 confirmed the loss of peroxisomes specifically in the periportal area (Fig. 2B,D). Furthermore, protein levels of peroxisomal membrane protein 70 (PMP70) and matrix protein catalase were decreased after 4 weeks of LPD (Fig. 3A,B). The observation of lower hepatic PMP70 protein levels already after 1 week of LPD (Fig. 3A) suggested that the loss of hepatic peroxisomes occurs at the early stages of protein malnutrition.

The loss of peroxisomes in the periportal region can be either due to a decrease in biogenesis or an increase in turnover. Peroxisomes are degraded by selective autophagy (pexophagy), which can be induced by amino acid deprivation [16]. This process requires concerted effort of autophagy receptors, p62/SQSTM1 and NBR1, which specifically bind and target peroxisomes for degradation [17]. However, accumulation of p62 is commonly seen in defective autophagy. Protein levels of autophagy marker LC3-II were elevated in liver after both 1 and 4 weeks of LPD, suggesting stimulation of autophagy. Levels of p62 were reduced after 1 week and elevated after 4 weeks in our LPD animals, the latter also being the case for NBR1 (Fig. S3A-G). The combined data suggests that autophagy is activated in our malnutrition model and that the loss of peroxisomes could be related to degradation. However, our data potentially indicates a block in autophagic flux after prolonged malnutrition. Prolonged starvation has also been shown to cause an elevation of p62 and NBR1 levels, which may contribute to the elevated levels observed after 4 weeks LPD [18]. Although we cannot rule out a role for impaired peroxisome biogenesis to explain the loss of peroxisomes in our LPD model, we did not observe changes in expression of genes involved in peroxisome biogenesis (see below).

Since β -oxidation of VLCFA takes place in peroxisomes, we analyzed hepatic VLCFA composition. Hepatic content of hexacosanoic (C26) (Fig. 3C) and docosatetraenoic acid (C22:4 ω 6) (Fig. 3D) as well as C26/C22 ratios (Fig. 3C) were increased in livers of LPD-fed animals, while the content of docosahexaenoic acid (C22:6 ω 3) was decreased (Fig. 3D). Similar changes in C26 and C22:6 ω 3 levels were reported in patients with Zellweger's syndrome [19], that lack functional peroxisomes. In agreement with patient data, plasma levels of di- and trihydroxycholestanoic acid (DHCA and THCA, respectively), bile acid intermediates that are metabolized by peroxisomal β -oxidation, were elevated in LPD-fed animals. Increased plasma

concentrations of unconjugated bile acids also pointed to a peroxisomal defect (Fig. 3E), as bile acid conjugation is a peroxisomal process [20].

Accumulation of deformed hepatic mitochondria in response to LPD

Further EM analysis revealed increased numbers of deformed mitochondria in livers of LPD-fed animals (Fig. 2C, Fig. S4). Mitochondria (in particular in zone 1) appeared enlarged with abnormal cristae, formed loops, contained inclusion bodies and increased numbers of mitochondrial granules. Immunofluorescence imaging of mitochondria substantiated the finding of enlarged and looped organelles in all hepatic zones of LPD-fed animals (Fig. 4), a phenomenon that has also been observed in cultured cells grown under amino acid deprivation conditions [21]. Furthermore, mitochondria elongation factor mitofusin-2 (Mfn2) was increased in isolated mitochondria from LPD-fed group (Fig. S3H). In addition, staining appeared more intense in the LPD-fed group suggesting an increased mitochondrial volume-density. This was confirmed by elevated relative mtDNA copy number and increased content of mitochondrial marker protein TOM20. However, in contrast to the early loss of peroxisomal markers, mitochondrial parameters were not yet altered after 1 week of LPD (Fig. 5A,B).

Hepatic mitochondrial function is severely impaired in LPD-fed rats

Next we determined whether changes in mitochondrial ultrastructure affected mitochondrial respiratory function. The basal oxygen consumption rates were not affected by the diet (Fig. 5C). In contrast, ADP-stimulated oxygen consumption rates (state 3) were lower in mitochondria from LPD-fed group (Fig. 5C). The strongest decrease was observed with pyruvate plus malate (PM), followed by palmitoyl-CoA plus L-carnitine plus malate (PCM) and succinate

plus pyruvate plus malate (SPM). This indicates impaired oxidative phosphorylation (OXPHOS) complex I activity, since dependence of oxygen flux on complex I activity is decreasing in the order PM>PCM>SPM. A milder impairment of oxygen consumption in the uncoupled state (Fig. 5C), in which ATP synthesis is inactivated due to dissipation of proton gradient, suggested both respiratory chain and ATP synthesis defects. Hepatic ATP content was indeed 40% reduced and AMP content was elevated (Fig. 6D), leading to strongly increased AMP/ATP ratio (Fig. 6D) and increased phosphorylation levels of AMP-activated protein kinase α subunit (AMPK α) (Fig. 5B). This implies that impaired mitochondrial ATP production was not compensated by increased mitochondrial mass.

Molecular underpinnings of LPD-induced mitochondrial dysfunction

To establish the molecular basis for LPD-induced mitochondrial dysfunction we determined protein levels and activities of enzymes involved in mitochondrial energy metabolism. There was a strong reduction in both OXPHOS complex I activity and level of Ndufb8 (Fig. 5D), which is needed for assembly and stability of complex I [22]. Complex IV activity and protein levels of subunit 1 were decreased as well in the LPD group (Fig. 5D). Proteomics analysis confirmed the strong effect of LPD on complex I and IV (Ndufs1 and Cox5a, respectively, Fig. S5B-C).

The observation that pyruvate-driven oxygen consumption rates were affected more than those driven by fatty acid (FA) substrate suggested that OXPHOS capacity is not the only factor that limited pyruvate oxidation. Proteomics showed that pyruvate dehydrogenase complex enzymes (Pdha1, Dlat and Dld) were not influenced by LPD (Fig. S5A). However, microarray data analysis revealed downregulation of mitochondrial pyruvate carrier subunit 1 (Mpc1 -1.47

fold, $p=0.016$), suggesting that pyruvate uptake, which has been shown to be rate limiting for pyruvate oxidation [23], was decreased under LPD conditions. Protein levels of other mitochondrial substrate transporters were also decreased (Fig. S5A), suggesting decreased supply of substrates for TCA cycle. This was accompanied by lower hepatic content of TCA cycle intermediates fumarate, malate and α -ketoglutarate, yet TCA cycle enzymes levels were not affected (Fig. 5E, Fig S5A).

The proteomic analysis of mitochondrial FAO enzymes showed that LPD had no effect on the carnitine palmitoyltransferase (Cpt) system that catalyzes acyl-CoA uptake into mitochondrial matrix (Fig. S5E), while three FAO enzymes, *i.e.*, medium-chain specific acyl-CoA dehydrogenase (Acadm), medium and short-chain L-3-hydroxyacyl-coenzyme A dehydrogenase (Hadh) and enoyl-CoA hydratase (Echs1), were decreased (Fig. 6E). In line with lower mitochondrial FAO capacity and the absence of peroxisomes, LPD caused accumulation of long-chain acyl-carnitines (C14-C18) (Fig. 5E). Moreover, the content of acetylcarnitine (C2) increased in the LPD-group (Fig. 5E), suggesting decreased utilization of acetyl-CoA in the TCA cycle leading to an increase in ketogenesis despite impaired FAO (Fig. 1C).

Steatosis and mitochondrial dysfunction has been linked to endoplasmic reticulum (ER) stress. Therefore markers of the 3 branches of the unfolded protein response (UPR) that is activated by ER stress [24] were analyzed next. In accordance with the transcriptomic data however, levels of both the transcription factors XBP1s and spliced ATF6 that initiate the 2 specific branches of the UPR remained similar to control animals, as well as their targets ERP72 and GRP78 (Fig. S5F-G). Increased eIF2 α phosphorylation and CHOP protein could be clearly observed though, strongly suggesting another form of stress. This is in line with data indicating that amino acid deprivation through GCN2 is activating the third branch also known as the

integrated stress response [24].

Microarray reveals transcriptional upregulation of major mitochondrial pathways without changes in peroxisomal gene expression

To gain further insight in the etiology of LPD-induced peroxisomal and mitochondrial alterations as well as the development of steatosis, liver transcriptome profiling was performed. Microarray data analysis revealed that 24% of the genes (4707 genes, FDR<5%) expressed in liver were differentially expressed after 4 weeks of LPD. Transcription factor network analysis showed enrichment of stress-induced transcription factor networks, including ATF3-5, HSF1 and CHOP, in line with our ER stress protein data (Table S4). Two targets of ATF4 were particularly upregulated, Tribbles3, a pseudokinase implicated in disrupting hepatic signaling pathways (33.6 fold), and fibroblast growth factor 21 (FGF21; up 13.5 fold), which is a central metabolic regulator induced by fasting [25].

The transcriptome analysis also revealed a lack of differential regulation of lipogenic transcription factor networks, including liver X receptor (LXR), sterol regulatory element-binding protein (SREBP), or peroxisome proliferator-activated receptor γ (PPAR γ), suggesting lipogenesis is not causing the steatosis, in line with the observed AMPK activation that regulates lipogenesis post-transcriptionally. Furthermore, there was no apparent downregulation of genes coding for peroxisomal FA oxidation, PMP70, or catalase in livers from LPD-fed animals. The expression of peroxisomal biogenesis genes was also not consistently changed, making it a less likely cause for reduced levels of peroxisomal proteins (Table S5).

Analysis of mitochondrial pathways revealed mitochondrial amino acid metabolism, TCA cycle, OXPHOS and β -oxidation among the pathways affected by LPD, while

mitochondrial organization emerged as the strongest enriched biological function (Fig. 5F) [26]. In line with increased mitochondrial content, the gene-set enrichment analysis suggested transcriptional upregulation of mitochondrial biogenesis in livers of LPD-fed animals as indicated by the enrichment of mitochondrial gene expression pathway ($p < 0.004$), which includes key regulator of mitochondrial biogenesis peroxisome proliferator-activated receptor gamma, coactivator 1 alpha (*Ppargc1a*, up 2.95 fold, $p = 0.0003$). Upregulation of mitochondrial proteases and chaperones indicated induction of quality control pathways (Table S6) and the presence of mitochondrial stress. Upregulation of mitofusin 1 (*Mfn1*) and downregulation of mitochondrial fission protein 1 (*Fis1*) (Table S6) was in agreement with the observation of elongated mitochondria. Together these data suggest that the observed mitochondrial functional impairments are in part mediated transcriptionally.

Fenofibrate reduces liver steatosis with restoration of peroxisomes, mitochondrial FAO, ATP content and albumin synthesis

To better understand the role of peroxisome and mitochondrial function on hepatic lipid metabolism we investigated whether activating peroxisome proliferator-activated receptor alpha (PPAR α), a nuclear receptor that stimulates peroxisome biogenesis and mitochondrial nutrient oxidation [27], may improve hepatic metabolic function. We aimed to test the PPAR α activator fenofibrate after a period of exposure to a malnutrition-inducing diet and development of steatosis. Treatment with fenofibrate for 2 weeks, while maintaining the animals on LPD, had no effect on the body weight, but it strongly reduced hepatic TG content and restored plasma albumin concentrations (Fig. 6A), suggesting improved liver function. Histology confirmed a reduction in hepatic steatosis (Fig. 6B). EM showed increased peroxisome numbers in the

hepatic periportal regions of fenofibrate-treated animals (Fig. 2E), that was confirmed by increased hepatic PMP70 protein levels (Fig. 6C). Although, PPAR- α activation has been shown to transcriptionally activate autophagy, we observed a decrease in LC3II with fenofibrate treatment. We therefore cannot rule out that, apart from increased biogenesis, the increase in peroxisome numbers is related to a downregulation of pexophagy.

Fenofibrate treatment had no effect on the mitochondrial density markers, i.e. hepatic TOM20 protein level and mtDNA copy number remained higher compared to 20% protein diet-fed controls (Fig. 6C-D). However, the treatment did improve mitochondrial morphology. Elongation was still commonly seen, but the occurrence of large deformed mitochondria with inclusions was decreased in response to fenofibrate treatment (Fig. 2E). Importantly, hepatic ATP content was restored with a concomitant reduction in the AMP/ATP ratio (Fig. 6E) and decreased phosphorylation levels of AMPK α (Fig. 6D), implying normalization of mitochondrial ATP production. Analysis of FAO intermediates revealed that fenofibrate treatment caused a nearly fourfold increase in the hepatic free carnitine content (C0) (Fig. 6E), which is required for mitochondrial acyl-CoA uptake. This is in agreement with previous reports showing both stimulation of hepatic carnitine biosynthesis and enhanced hepatic carnitine uptake in response to PPAR α activation [28]. The content of long-chain acylcarnitines (C14-C18) (Fig. 6E), in particular C18 species (Fig. S6F), was strongly increased after fenofibrate treatment. This suggested that the supply exceeded mitochondrial FAO capacity, which was also strongly increased as indicated by nearly 45% higher oxygen consumption rate in the coupled (Fig. 6F) and uncoupled states (Fig. S6B) and slightly higher basal oxygen consumption rate (Fig. S6A) with FA substrate palmitoyl-CoA. Pyruvate-driven oxygen consumption rates were minimally affected by fenofibrate treatment (Fig. 6F, Fig. S6A-B), as well as OXPHOS complexes,

including complex I (Ndufb8 and Ndufs1) and complex IV (Cox5A, Fig. S5C, S6D-E). Moreover, complex I activity was not restored by the activation of PPAR α (Fig. S6C).

The differential effect of fenofibrate on the FA *versus* pyruvate oxidation in combination with the lack of effect on OXPHOS indicates that the restoration of FAO by fenofibrate occurs upstream of OXPHOS, *i.e.*, of enzymes and transporters that are not involved in pyruvate oxidation. Indeed, proteomics (Fig. 6G, Fig. S5E) showed massive upregulation of mitochondrial FAO enzymes, including Cpt1a, which controls β -oxidation flux [29], and Acadm and Hadh both of which were decreased in response to LPD.

Discussion

Severe malnutrition is associated with a high risk of mortality related to severe metabolic disturbances. But, despite its widespread prevalence, in-depth understanding of the pathophysiological processes is lacking. In this study we present an in depth examination of the hepatic cellular and metabolic pathology in an animal model of severe malnutrition. We show that a LPD in weanling animals causes severe periportal hepatic steatosis along with the loss of peroxisomes and impaired mitochondrial function. Mitochondria showed multiple functional defects including a decrease in Complex I and complex IV activity, and impaired mitochondrial pyruvate and FA oxidation, resulting in a profound hepatic energy deficit, despite an increase in mitochondrial abundance (see model, Figure 7). Strikingly, activation of nuclear receptor PPAR α restored hepatic peroxisomal content and increased mitochondrial FAO capacity but it did not rescue either respiratory chain defects or pyruvate oxidation capacity. The PPAR α induction of peroxisomal biogenesis and stimulation of mitochondrial FAO was sufficient to ameliorate hepatic steatosis and remarkably restore hepatic energy status and albumin synthesis suggesting a link between the peroxisomal and mitochondrial dysfunction, and liver health during malnutrition. Our study expands the understanding of early observations that suggested impairment of mitochondrial bioenergetic functions in livers of severely malnourished rats [30, 31] and humans [32] and postulated a link between the loss of peroxisomal function and development of a fatty liver in severe malnutrition [33]

Translating the animal model to the clinical phenotype of malnutrition

Two clinical phenotypes of severe malnutrition exist. Marasmus is defined by clinical wasting, while kwashiorkor is typically accompanied by more complex characteristics such as

pitting edema, hair discoloration, skin lesions and hepatomegaly, although considerable overlap with marasmus often exists. Biochemical features typically present in kwashiorkor include hepatic steatosis [34, 35], a reduced protein turnover [36] and decreased albumin synthesis [37]. The plasma concentrations of antioxidants are generally lower, while the levels of oxidative stress markers are elevated [7, 38]. Our malnutrition animal model displayed both signs of marasmus (wasting) and hallmarks of kwashiorkor (hypoalbuminemia and hepatic steatosis). However, the model lacked other specific clinical features of kwashiorkor such as edema and skin lesions. It is possible that the dietary protein levels used in our model were too high to observe these phenotypes as a lower protein concentration in the diet was reported to generate both edema and skin lesions [39]. However, dietary protein deficiency is probably not the only factor needed to elicit features of kwashiorkor as similar nutritional intake in terms of quantity and composition has been observed in children with kwashiorkor and marasmus [40]. Our animal model consisted of feeding a low protein diet, replacing the protein with additional complex carbohydrates, while maintaining the same 35% of sucrose by chow weight for both the low protein and control diet. We aimed to mimic what is generally observed in the developing countries where staple food such as maize or cassava is generally low in protein and high in carbohydrates. The diet also often has a substantial amount of refined sugar. Interestingly one of the first hypotheses generated to explain the pathophysiology of kwashiorkor implicated carbohydrates to be involved in the pathogenesis and it is tempting to speculate that the combination of a diet deficient in protein but high in carbohydrates also contributed to the hepatic phenotype seen in our model [41]. Previous studies, including in a non-primate monkey model [42], also suggested that the combination of low protein and high carbohydrates was able to induce the specific pathophysiological phenotype.

Comparing malnutrition-induced hepatic metabolic dysfunction with non-alcoholic fatty liver disease

Severe malnutrition as well as overfeeding and obesity can cause hepatic steatosis and mitochondrial changes, which in the context of obesity is known as non-alcoholic fatty liver disease (NAFLD). Enlarged mitochondria with abnormal cristae and intracristalline structures have been observed in NAFLD; in our model we found mitochondrial inclusion bodies [43]. NAFLD has been found to be associated with increased mitochondrial mass [13,44], although liver mtDNA was decreased in a study using livers from NAFLD patients [45]. Reduced complex I activity has been found in NAFLD [46], although not consistently [reviewed in 9]. Of note, choline deficient diet-induced steatosis also causes reduced complex I activity [47]. Since impaired complex I activity is found both in NAFLD and in our LPD model, one might speculate that hepatic lipid accumulation is the cause rather than the effect of the reduced complex I activity. However, our finding that complex I activity is not restored by fenofibrate treatment, while hepatic lipid content is reduced, suggests that the impairment of complex I is a direct result of LPD. Some changes in our model are not typically found in NAFLD. For example, despite mitochondrial damage, a higher lipid oxidation rate has been observed in NAFLD patients [See review 9], which was found to be reduced in our model. There is very limited data on the role of peroxisomes in NAFLD. A few studies suggested an increased peroxisome content in NAFLD [46,48], indicating that the loss of peroxisomes is specific for malnutrition-related steatosis. Detailed metabolic analyses in NAFLD does indicate certain similarities with our model, including the effects on the TCA cycle [49,50]. The effect of fenofibrate in increasing the long-chain acylcarnitines in our model is intriguing. It has been demonstrated that at least for muscle,

obesity-induced mitochondria overload causes accumulation of intermediates that subsequently induces insulin resistance and not so much a total defect in oxidation as is often claimed [51]. Fibrates have been proposed in the treatment of NAFLD but some authors found a negative outcome [52]. As signs of incomplete oxidation are exacerbated by fenofibrate, long term treatment could be ineffective, or even aggravate hepatic metabolic dysfunction, as was also proposed [52].

Mechanisms for the malnutrition-induced loss of peroxisomes

In the present study peroxisomal structural and functional alterations were not accompanied by decreased expression of peroxisome biogenesis genes. Instead, the increase in autophagy markers along with autophagy receptors involved in autophagic degradation of peroxisomes suggests that the loss of peroxisomes is likely due to an increase in pexophagy and not the reduction of biogenesis. Amino acid deprivation is a potent inductor of pexophagy [16]. The livers of starved mice have been reported to lose over 40% of their protein content within 48 hours [16]. Thus it is not surprising that peroxisomes are selectively degraded during starvation as they are very protein-dense structures within a cell and likely less critical for immediate survival of hepatocytes. Yet, the induction of pexophagy during a prolonged period of starvation may be detrimental, since peroxisomes prevent the accumulation of bile acid intermediates that can be toxic to the liver [53]. Indeed, loss of peroxisomes observed in the present study was accompanied by increased plasma levels of unconjugated C24 bile acids, possibly contributing to hepatic toxicity and damage

The relation between peroxisomal and mitochondrial function

Although we could not directly demonstrate that the loss of peroxisomes resulted in impaired mitochondria function, there is evidence to support this hypothesis. The importance of peroxisomes for mitochondria fitness was initially described in the first report of peroxisome biogenesis disorder where individuals lacking detectable peroxisomes showed clear signs of dysfunctional and deformed mitochondria [54]. Interestingly, animal models with genetic deficiencies in peroxisomal biogenesis showed mitochondrial disturbances that were similar to those observed in our malnutrition model such as lower complex I activity [12, 55]. There is some evidence showing that the loss of peroxisomal redox regulation may negatively affect the redox status of mitochondria, resulting in an increase in mitochondria oxidative stress [56]. Furthermore, the loss of peroxisomal VLCFA β -oxidation activity results in the impairment of mitochondrial OXPHOS and mitochondria damage [57, 58], albeit the underlying mechanism is unknown. In analogue to the peroxisomal defect disease models, we observed in our malnutrition model decreased numbers of peroxisomes (Fig. 3A), an increase in oxidative stress (Fig. 1D), the accumulation of VLCFA (Fig. 3C) and a decrease in OXPHOS capacity (Fig. 5C). Together these results suggest that the loss of peroxisomes and mitochondrial dysfunction during prolonged malnutrition may be responsible for some of hepatic metabolic defects observed in our animal model. This notion is further supported by the fact that treatment with PPAR α agonist fenofibrate resulted in a concerted reappearance of peroxisomes and normalization of mitochondrial morphology and function, leading to amelioration of hepatic phenotype.

Conclusions

This study is unique in its comprehensive approach to understand the complex hepatic metabolic consequences of severe malnutrition. It is the first study to demonstrate a diet induced

loss of peroxisomes *in vivo*. The results of this study could potentially lead to novel treatment strategies for severely malnourished children. For example, numerous studies have shown that hypoalbuminemia is strongly associated with increased mortality in critically sick patients [59]. Interventions aimed at restoring hepatic mitochondrial function and thereby raising serum albumin levels could lead to improved clinical outcome of severely malnourished children. Since polyunsaturated FA, such as linoleic and docosahexaenoic acid are strong natural ligands of PPAR α [60], it would be interesting to evaluate whether dietary supplementation with these FA in the early phases of treatment would improve hepatic function and clinical outcome of severely malnourished children.

References

Author names in bold designate shared co-first authorship

- [1] Black RE, Victora CG, Walker SP, Bhutta ZA, Christian P, de Onis M, et al. Maternal and child undernutrition and overweight in low-income and middle-income countries. *Lancet* 2013;382:427-451.
- [2] WHO. Management of severe malnutrition: a manual for physicians and other senior health workers. Geneva: World Health Organization. Guideline 1999.
- [3] Heikens GT. How can we improve the care of severely malnourished children in Africa? *PLoS Med* 2007;4:e45.
- [4] Maitland K, Berkley JA, Shebbe M, Peshu N, English M, Newton CR. Children with severe malnutrition: can those at highest risk of death be identified with the WHO protocol? *PLoS Med* 2006;3:e500.
- [5] Waterlow JC. Protein-energy malnutrition. (London: Edward Arnold) 1992.
- [6] Leite HP, de Lima LF, de Oliveira Iglesias SB, Pacheco JC, de Carvalho WB. Malnutrition may worsen the prognosis of critically ill children with hyperglycemia and hypoglycemia. *JPEN J Parenter Enteral Nutr* 2013;37:335-341.
- [7] Manary MJ, Leeuwenburgh C, Heinecke JW. Increased oxidative stress in kwashiorkor. *J Pediatr* 2000;137:421-424.
- [8] **Smith MI, Yatsunenko T**, Manary MJ, Trehan I, Mkakosya R, Cheng J, et al. Gut microbiomes of Malawian twin pairs discordant for kwashiorkor. *Science* 2013;339:548-554.
- [9] **Begrache K, Massart J**, Robin MA, Bonnet F, Fromenty B. Mitochondrial adaptations and dysfunctions in nonalcoholic fatty liver disease. *Hepatology* 2013;58:1497-1507.
- [10] Smith JJ, Aitchison JD. Peroxisomes take shape. *Nat Rev Mol Cell Biol* 2013;14:803-

817.

- [11] Schrader M, Grille S, Fahimi HD, Islinger M. Peroxisome interactions and cross-talk with other subcellular compartments in animal cells. *Subcell Biochem* 2013;69:1-22.
- [12] Dirkx R, Vanhorebeek I, Martens K, Schad A, Grabenbauer M, Fahimi D, et al. Absence of peroxisomes in mouse hepatocytes causes mitochondrial and ER abnormalities. *Hepatology* 2005;41:868-878.
- [13] Koliaki C, Szendroedi J, Kaul K, Jelenik T, Nowotny P, Jankowiak F, et al. Adaptation of hepatic mitochondrial function in humans with non-alcoholic fatty liver is lost in steatohepatitis. *Cell Metab* 2015;21:739-746.
- [14] Bandsma RH, Mendel M, Spoelstra MN, Reijngoud DJ, Boer T, Stellaard F, et al. Mechanisms behind decreased endogenous glucose production in malnourished children. *Pediatr Res* 2010;68:423-428.
- [15] Rao DR, Deodhar AD, Hariharan K. Histidine metabolism in experimental protein malnutrition in rats. *Biochem J*. 1965 Oct;97(1):311-7.
- [16] Nordgren M, Wang B, Apanasets O, Fransen M. Peroxisome degradation in mammals: mechanisms of action, recent advances, and perspectives. *Front Physiol* 2013;4:145.
- [17] Deosaran E, Larsen KB, Hua R, Sargent G, Wang Y, Kim S, et al. NBR1 acts as an autophagy receptor for peroxisomes. *J Cell Sci* 2013;126:939-952.
- [18] Sahani MH, Itakura E, Mizushima N. Expression of the autophagy substrate SQSTM1/p62 is restored during prolonged starvation depending on transcriptional upregulation and autophagy-derived amino acids. *Autophagy*. 2014;10:431-441.
- [19] Martinez M. Severe deficiency of docosahexaenoic acid in peroxisomal disorders: a defect of delta 4 desaturation? *Neurology* 1990;40:1292-1298.

- [20] **Keane MH, Overmars H**, Wikander TM, Ferdinandusse S, Duran M, Wanders RJ, et al. Bile acid treatment alters hepatic disease and bile acid transport in peroxisome-deficient PEX2 Zellweger mice. *Hepatology* 2007;45:982-997.
- [21] Gomes LC, Di Benedetto G, Scorrano L. During autophagy mitochondria elongate, are spared from degradation and sustain cell viability. *Nat Cell Biol* 2011;13:589-598.
- [22] Lazarou M, Thorburn DR, Ryan MT, McKenzie M. Assembly of mitochondrial complex I and defects in disease. *Biochim Biophys Acta* 2009;1793:78-88.
- [23] Schell JC, Rutter J. The long and winding road to the mitochondrial pyruvate carrier. *Cancer Metab* 2013;1:6.
- [24] Ron D, Walter P. Signal integration in the endoplasmic reticulum unfolded protein response. *Nat Rev Mol Cell Biol*. 2007;8:519-529.
- [25] Liang Q, Zhong L, Zhang J, Wang Y, Bornstein SR, Triggle CR, et al. FGF21 maintains glucose homeostasis by mediating the cross talk between liver and brain during prolonged fasting. *Diabetes* 2014;63:4064-4075.
- [26] **Huang da W, Sherman BT**, Lempicki RA. Systematic and integrative analysis of large gene lists using DAVID bioinformatics resources. *Nat Protoc* 2009;4:44-57.
- [27] Kersten S, Seydoux J, Peters JM, Gonzalez FJ, Desvergne B, Wahli W. Peroxisome proliferator-activated receptor alpha mediates the adaptive response to fasting. *J Clin Invest* 1999;103:1489-1498.
- [28] van Vlies N, Ferdinandusse S, Turkenburg M, Wanders RJ, Vaz FM. PPAR alpha-activation results in enhanced carnitine biosynthesis and OCTN2-mediated hepatic carnitine accumulation. *Biochim Biophys Acta* 2007;1767:1134-1142.
- [29] Spurway TD, Sherratt HA, Pogson CI, Agius L. The flux control coefficient of carnitine

palmitoyltransferase I on palmitate beta-oxidation in rat hepatocyte cultures. *Biochem J* 1997;323 (Pt 1):119-122.

[30] Ferreira J, Gil L. Nutritional effects on mitochondrial bioenergetics. Alterations in oxidative phosphorylation by rat liver mitochondria. *Biochem J* 1984;218:61-67.

[31] Olowookere JO, Olorunsogo OO, Malomo SO. Effects of defective in vivo synthesis of mitochondrial proteins on cellular biochemistry and physiology of malnourished rats. *Ann Nutr Metab* 1990;34:147-154.

[32] Waterlow JC. Oxidative phosphorylation in the livers of normal and malnourished human infants. *Proc R Soc Lond B Biol Sci* 1961;155:96-114.

[33] Doherty JF, Golden MH, Brooks SE. Peroxisomes and the fatty liver of malnutrition: an hypothesis. *Am J Clin Nutr* 1991;54:674-677.

[34] McLean AE. Hepatic failure in malnutrition. *Lancet* 1962;2:1292-1294.

[35] Williams CD. A nutritional disease of childhood associated with a maize diet. *Arch Dis Child* 1933;8:423-433.

[36] Jahoor F, Badaloo A, Reid M, Forrester T. Protein kinetic differences between children with edematous and nonedematous severe childhood undernutrition in the fed and postabsorptive states. *Am J Clin Nutr* 2005;82:792-800.

[37] Morlese JF, Forrester T, Badaloo A, Del Rosario M, Frazer M, Jahoor F. Albumin kinetics in edematous and nonedematous protein-energy malnourished children. *Am J Clin Nutr* 1996;64:952-959.

[38] Fechner A, Bohme C, Gromer S, Funk M, Schirmer R, Becker K. Antioxidant status and nitric oxide in the malnutrition syndrome kwashiorkor. *Pediatr Res* 2001;49:237-243.

[39] Edozien JC. Experimental kwashiorkor and marasmus. *Nature* 1968;220:917-919.

- [40] Sullivan J, Ndekha M, Maker D, Hotz C, Manary MJ. The quality of the diet in Malawian children with kwashiorkor and marasmus. *Matern Child Nutr* 2006;2:114-122.
- [41] Whitehead RG, Alleyne GA. Pathophysiological factors of importance in protein-calorie malnutrition. *Br Med Bull* 1972;28:72-79.
- [42] Coward WA, Whitehead RG. Changes in haemoglobin concentrations during the development of kwashiorkor. *Br J Nutr.* 1972;28:463-471.
- [43] Sanyal AJ, Campbell-Sargent C, Mirshahi F, Rizzo WB, Contos MJ, Sterling RK, et al. Nonalcoholic steatohepatitis: association of insulin resistance and mitochondrial abnormalities. *Gastroenterology* 2001;120:1183-1192.
- [44] **Carabelli J, Burgueño AL**, Rosselli MS, Gianotti TF, Lago NR, Pirola CJ, Sookoian S. High fat diet-induced liver steatosis promotes an increase in liver mitochondrial biogenesis in response to hypoxia. *J Cell Mol Med* 2011;15:1329-1338.
- [45] Sookoian S, Rosselli MS, Gemma C, Burgueño AL, Fernández Gianotti T, Castaño GO, Pirola CJ. Epigenetic regulation of insulin resistance in nonalcoholic fatty liver disease: impact of liver methylation of the peroxisome proliferator-activated receptor γ coactivator 1 α promoter. *Hepatology* 2010;52:1992-2000.
- [46] Pirola CJ, Gianotti TF, Burgueño AL, Rey-Funes M, Loidl CF, Mallardi P, et al. Epigenetic modification of liver mitochondrial DNA is associated with histological severity of nonalcoholic fatty liver disease. *Gut* 2013;62:1356-1363.
- [47] Petrosillo G, Portincasa P, Grattagliano I, Casanova G, Matera M, Ruggiero FM, et al. Mitochondrial dysfunction in rat with nonalcoholic fatty liver Involvement of complex I, reactive oxygen species and cardiolipin. *Biochim Biophys Acta* 2007;1767:1260-1267.
- [48] Knebel B, Hartwig S, Haas J, Lehr S, Goeddeke S, Susanto F, et al. Peroxisomes

compensate hepatic lipid overflow in mice with fatty liver. *Biochim Biophys Acta*. 2015;1851:965-976.

[49] Sookoian S, Castaño GO, Scian R, Fernández Gianotti T, Dopazo H, Rohr C, et al. Serum aminotransferases in nonalcoholic fatty liver disease are a signature of liver metabolic perturbations at the amino acid and Krebs cycle level. *Am J Clin Nutr*. 2016;103:422-434.

[50] Sunny NE, Kalavalapalli S, Bril F, Garrett TJ, Nautiyal M, Mathew JT, et al. Cross-talk between branched-chain amino acids and hepatic mitochondria is compromised in nonalcoholic fatty liver disease. *Am J Physiol Endocrinol Metab*. 2015;309:E311-3119.

[51] Muoio DM, Neufer PD. Lipid-induced mitochondrial stress and insulin action in muscle. *Cell Metab* 2012;15:595-605.

[52] Yan F, Wang Q, Xu C, Cao M, Zhou X, Wang T, et al. Peroxisome Proliferator-Activated Receptor α Activation Induces Hepatic Steatosis, Suggesting an Adverse Effect. *PLoS One* 2014;9:e99245.

[53] Woolbright BL, Jaeschke H. Novel insight into mechanisms of cholestatic liver injury. *World J Gastroenterol* 2012;18:4985-4993.

[54] Braverman NE, D'Agostino MD, Maclean GE. Peroxisome biogenesis disorders: Biological, clinical and pathophysiological perspectives. *Dev Disabil Res Rev* 2013;17:187-196.

[55] Baumgart E, Vanhorebeek I, Grabenbauer M, Borgers M, Declercq PE, Fahimi HD, et al. Mitochondrial alterations caused by defective peroxisomal biogenesis in a mouse model for Zellweger syndrome (PEX5 knockout mouse). *Am J Pathol* 2001;159:1477-1494.

[56] Ivashchenko O, Van Veldhoven PP, Brees C, Ho YS, Terlecky SR, Fransen M. Intraperoxisomal redox balance in mammalian cells: oxidative stress and interorganellar cross-talk. *Mol Biol Cell* 2011;22:1440-1451.

- [57] **Fourcade S, Lopez-Erauskin J**, Ruiz M, Ferrer I, Pujol A. Mitochondrial dysfunction and oxidative damage cooperatively fuel axonal degeneration in X-linked adrenoleukodystrophy. *Biochimie* 2014;98:143-149.
- [58] Lopez-Erauskin J, Galino J, Ruiz M, Cuezva JM, Fabregat I, Cacabelos D, et al. Impaired mitochondrial oxidative phosphorylation in the peroxisomal disease X-linked adrenoleukodystrophy. *Hum Mol Genet* 2013;22:3296-3305.
- [59] Jellinge ME, Henriksen DP, Hallas P, Brabrand M. Hypoalbuminemia is a strong predictor of 30-day all-cause mortality in acutely admitted medical patients: a prospective, observational, cohort study. *PLoS One* 2014;9:e105983.
- [60] Keller H, Dreyer C, Medin J, Mahfoudi A, Ozato K, Wahli W. Fatty acids and retinoids control lipid metabolism through activation of peroxisome proliferator-activated receptor-retinoid X receptor heterodimers. *Proc Natl Acad Sci U S A* 1993;90:2160-2164.

Figure legends

Figure 1. Severe growth failure and hepatic steatosis in LPD-fed rats. (A) Growth curves. (B) Food intake. (C) Plasma triglyceride, albumin, alanine-transaminase, lactate, β -hydroxybutyrate and fasting glucose concentrations. (D) Liver weights, body weight-normalized liver weights, hepatic triglycerides, glycogen and thiobarbituric acid reactive substances (TBARS). Data are means from N=6 animals per diet group; \pm SD. * $p < 0.05$, ** $p < 0.001$ compared to 20% protein diet group.

Figure 2. LPD induces changes in hepatic peroxisomal distribution (A) Electron micrograph of periportal hepatocyte from a control animal, showing a peroxisome (arrow) and numerous mitochondria. (B) Immunofluorescent staining of peroxisome marker PEX14 (red) of liver periportal area from a control animal, with nuclei in blue. (C) Electron micrograph of periportal hepatocyte from LPD-fed animal. Note the absence of peroxisomes, presence of electron opaque lipid and numerous abnormal mitochondria. (D) Pex14 staining of periportal area of liver in LPD-fed animal, showing decreased signal. (E) Periportal area of liver from a fenofibrate treated animal. Mitochondria morphology has improved and peroxisomes have reappeared (arrows). (F) Pex14-stained perivenous area of liver in LPD-fed animal.

Figure 3. LPD causes loss of peroxisomal proteins and increases levels of biochemical markers indicating peroxisomal dysfunction. (A) Protein levels of Pmp70 in livers. (B) Protein levels of catalase in livers. (C) Hepatic content of hexacosanoic acid (C26:0) and the ratios of C24/C22, C25/C22 and C26/C22 in livers. (D) Hepatic polyunsaturated fatty acid

profile. (E) Plasma bile acid and bile acid intermediate profiles. Data are means from N=6-8 animals per experimental group; \pm SD. * p <0.05 and ** p <0.001 compared to 20% protein diet group.

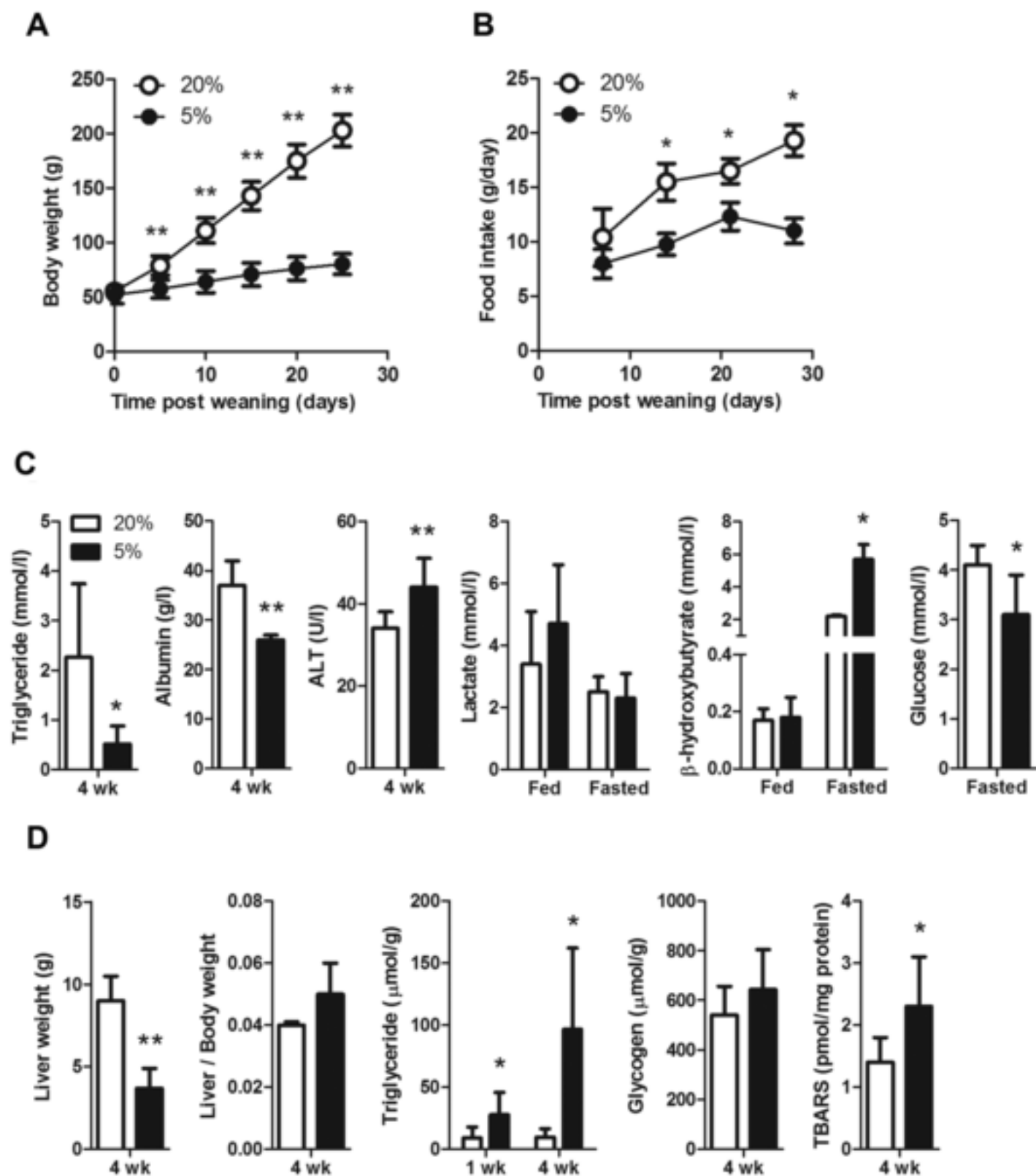
Figure 4. LPD induces formation of deformed and elongated mitochondria. Fluorescent immunohistochemistry of mitochondrial Hsp60 (red) in liver sections in (A,B) periportal and (C,D) perivenous area. Panels below are zoomed sections of the area indicated in the corresponding panels above. Size bar equals 10 μ m.

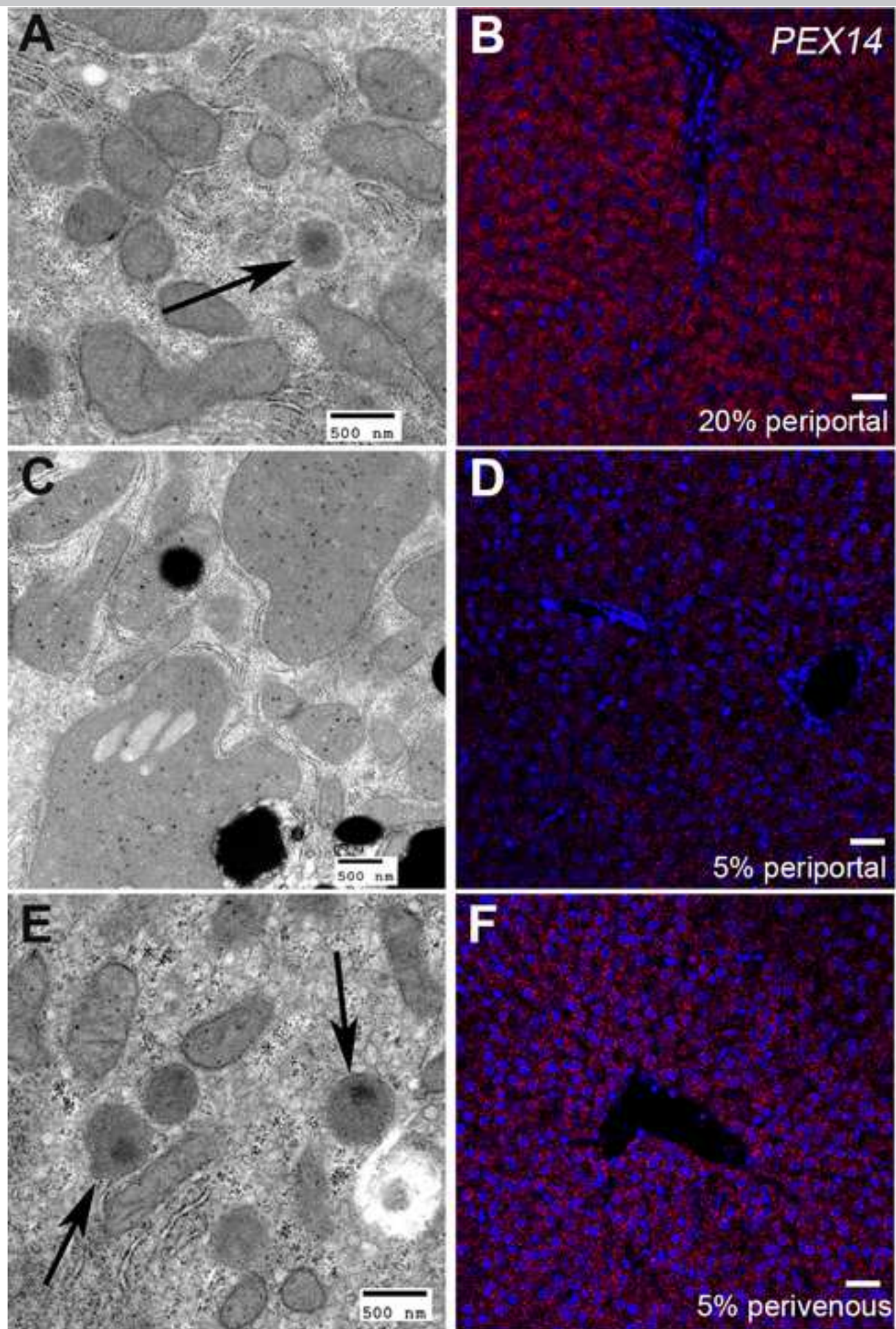
Figure 5. LPD feeding results in multiple mitochondrial defects. (A) Relative hepatic mtDNA copy number. (B) Hepatic TOM20, AMPK α immunoblots and quantification. (C) O₂ flux in state-4, state-3 and state-U in isolated mitochondria oxidizing pyruvate+malate (PM), succinate+pyruvate+malate (SPM) and palmitoyl-CoA+L-carnitine+malate (PCM). (D) Isolated mitochondria OXPHOS-(I-V) complex activities and levels in. (E) Hepatic TCA cycle intermediates, free carnitine and acylcarnitines (F) Top-10 KEGG pathway and biological process-based categories of 694 differentially expressed (FDR 10%-ranked) genes coding for mitochondrial proteins after 4 weeks of low protein diet. N=5-6, except for adenosine(mono-/di-/tri-)phosphates; N=3; \pm SD. ** p <0.001 and * p <0.05 compared to 20% protein diet group after 4 weeks of diet. ++ p <0.001 and ^^ p <0.001 compared to 20% and 5% protein diet group after 1 week of diet, respectively.

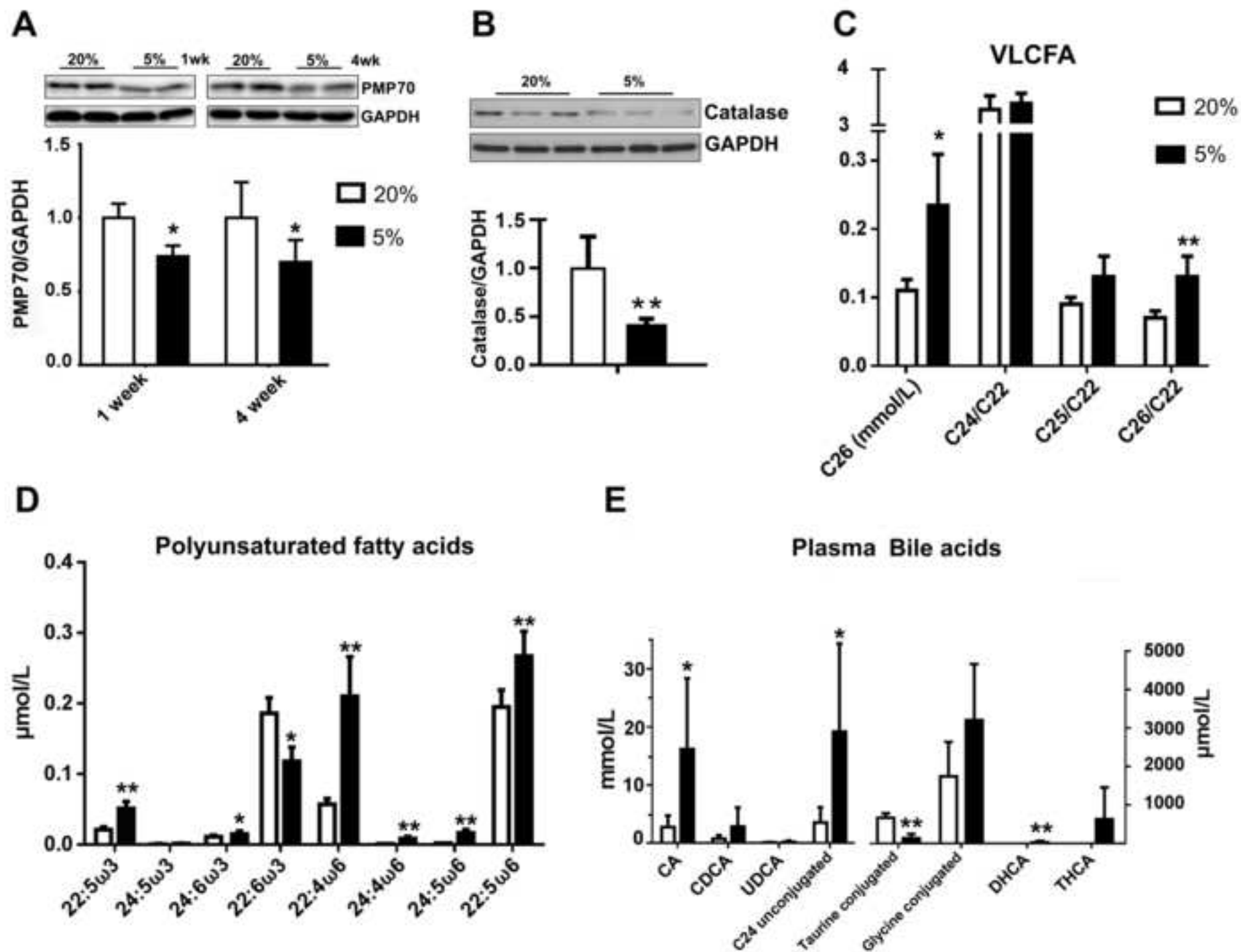
Figure 6. Fenofibrate treatment ameliorates LPD-induced hepatic phenotype. (A) Body weight, hepatic triglycerides, plasma albumin. (B) Low power haematoxylin and eosin (H&E) stained liver sections of an untreated and fenofibrate (FF) treated malnourished animal. (C)

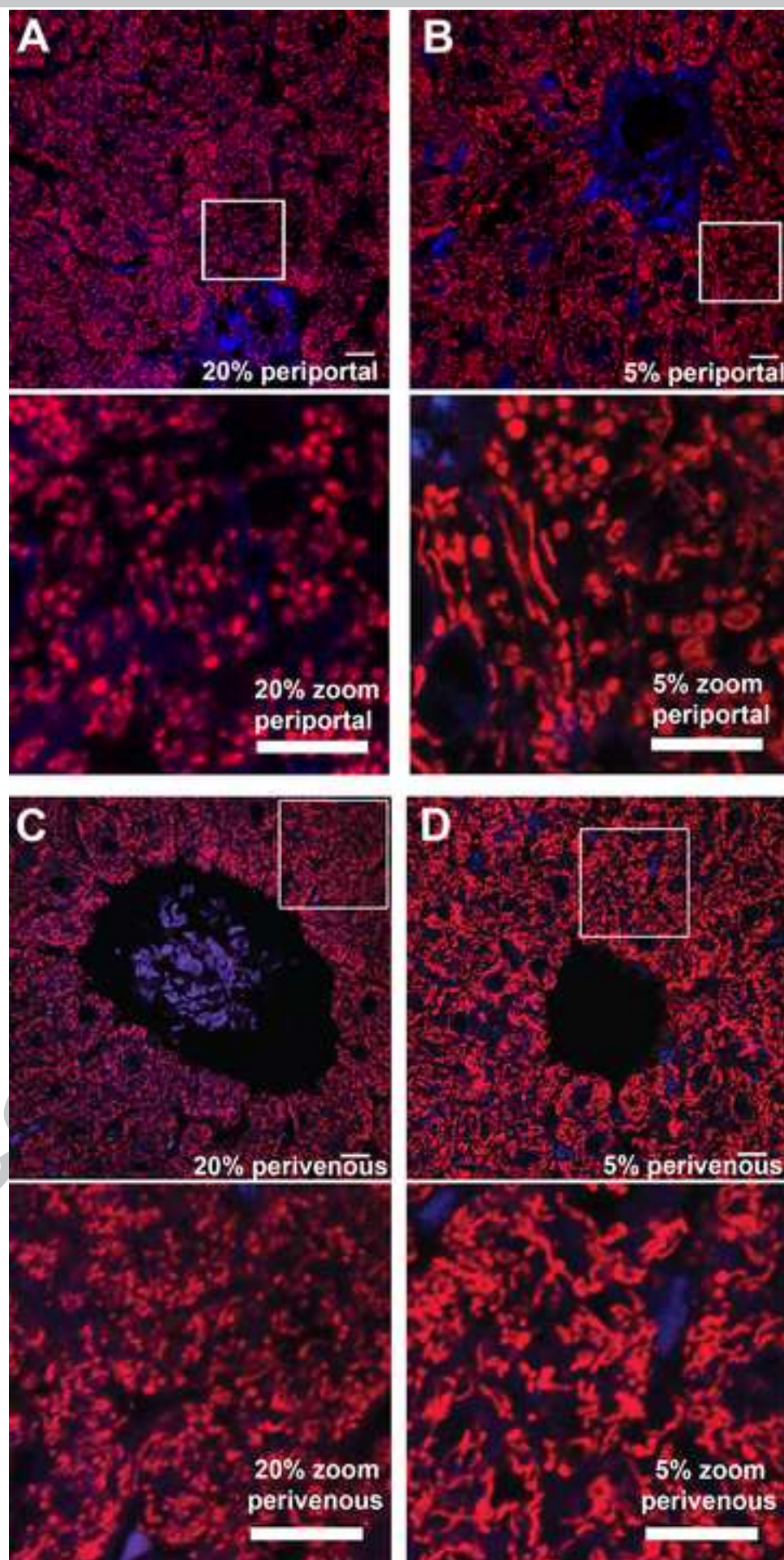
Relative hepatic mtDNA copy number. **(D)** Protein levels and quantification of PMP70, TOM20 and phosphorylated AMPK α in liver. **(E)** Hepatic ATP, ADP, AMP, AMP/ATP ratio and free carnitine (C0), acetylcarnitine (C2) and long-chain acylcarnitines (C14-C18) content. **(F)** O₂ flux in state-3 in isolated liver mitochondria oxidizing pyruvate+malate (PM) and palmitoyl-CoA+L-carnitine+malate (PCM), **(G)** Targeted quantitative proteomics of mitochondrial β -oxidation enzymes in isolated mitochondria, indicated by UniProt accession number and gene name. N=5-6, \pm SD. **p<0.001 and *p<0.05 compared to 20%, ^{##}p<0.001 and [#]p<0.05 compared to 5% protein diet group.

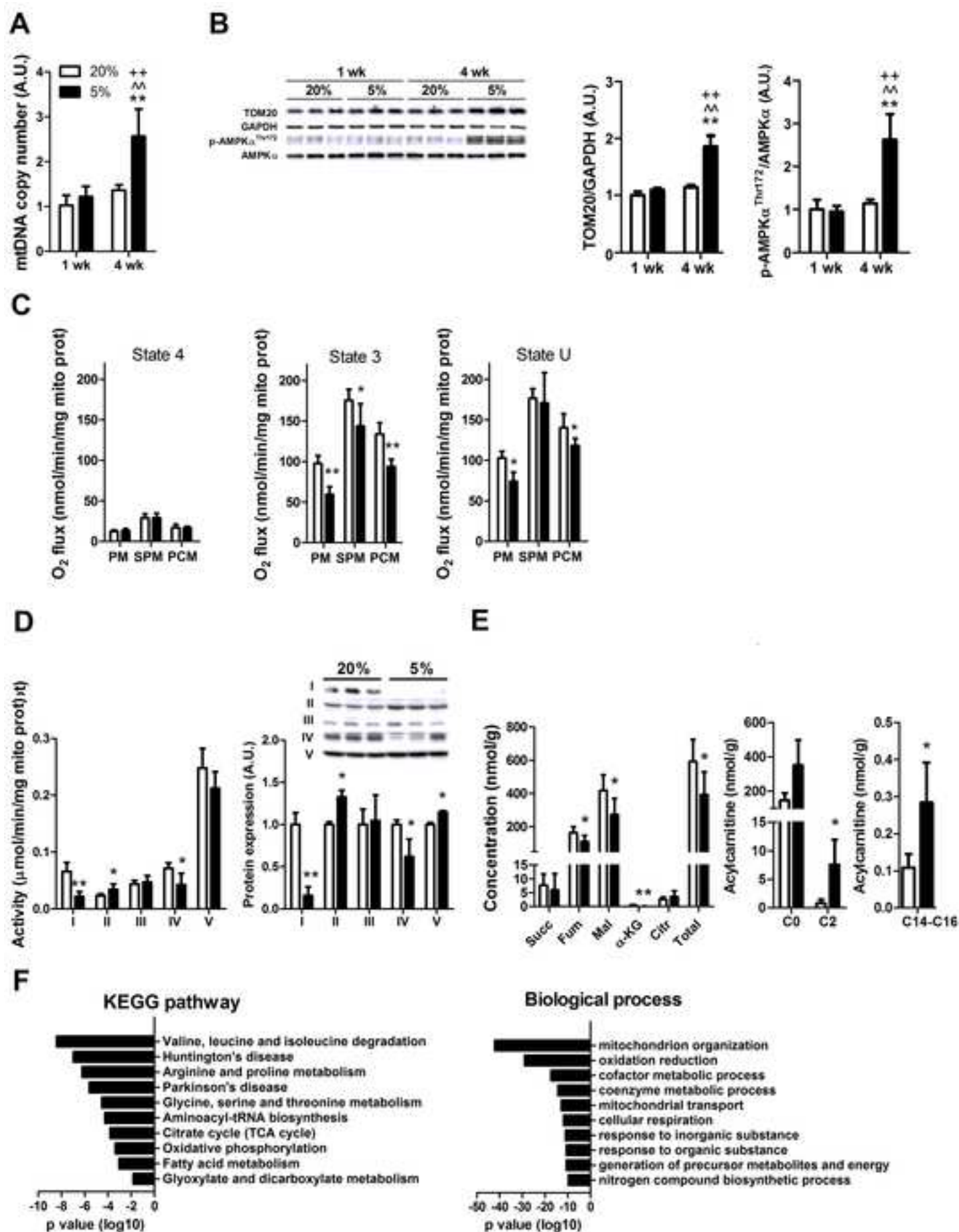
Figure 7. Model of LPD-induced loss of hepatic peroxisomes and mitochondrial dysfunction. Loss of peroxisomes leads to altered bile acid synthesis and metabolism and impaired oxidation of very long-chain fatty acids, whereas mitochondrial dysfunction is characterized by impaired oxidative phosphorylation, TCA cycle and β -oxidation. Together these defects cause hepatic steatosis and ATP deficit.

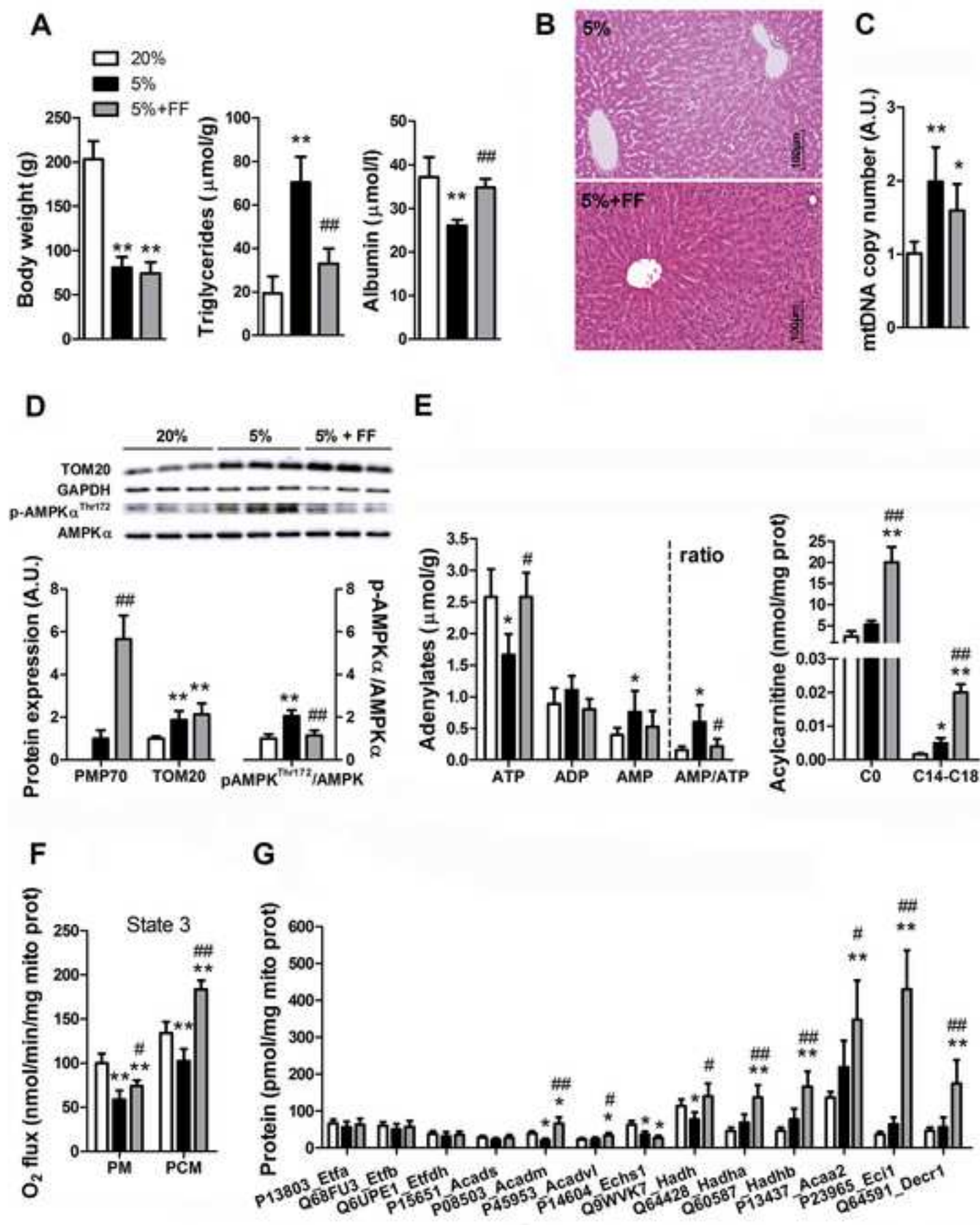


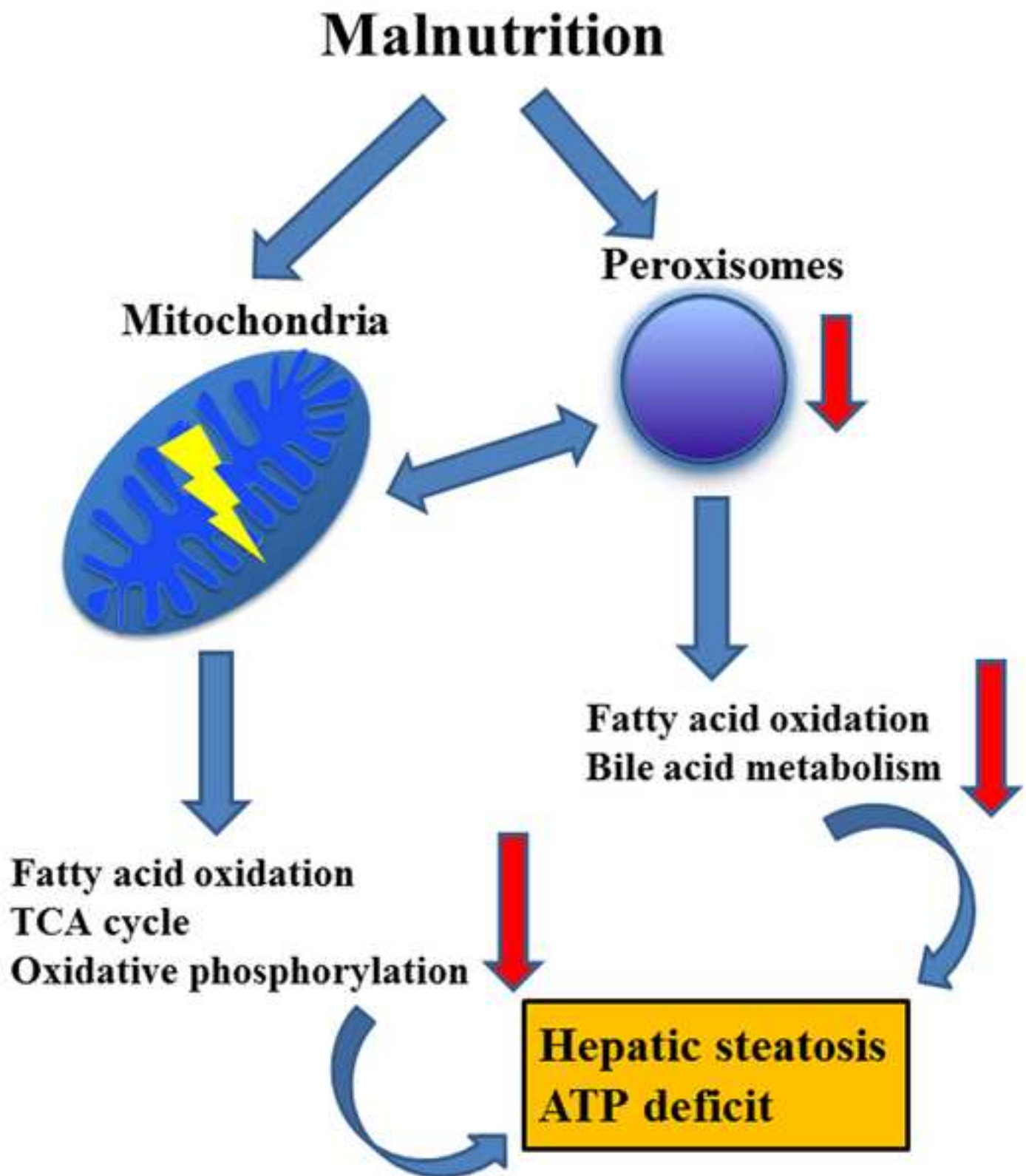


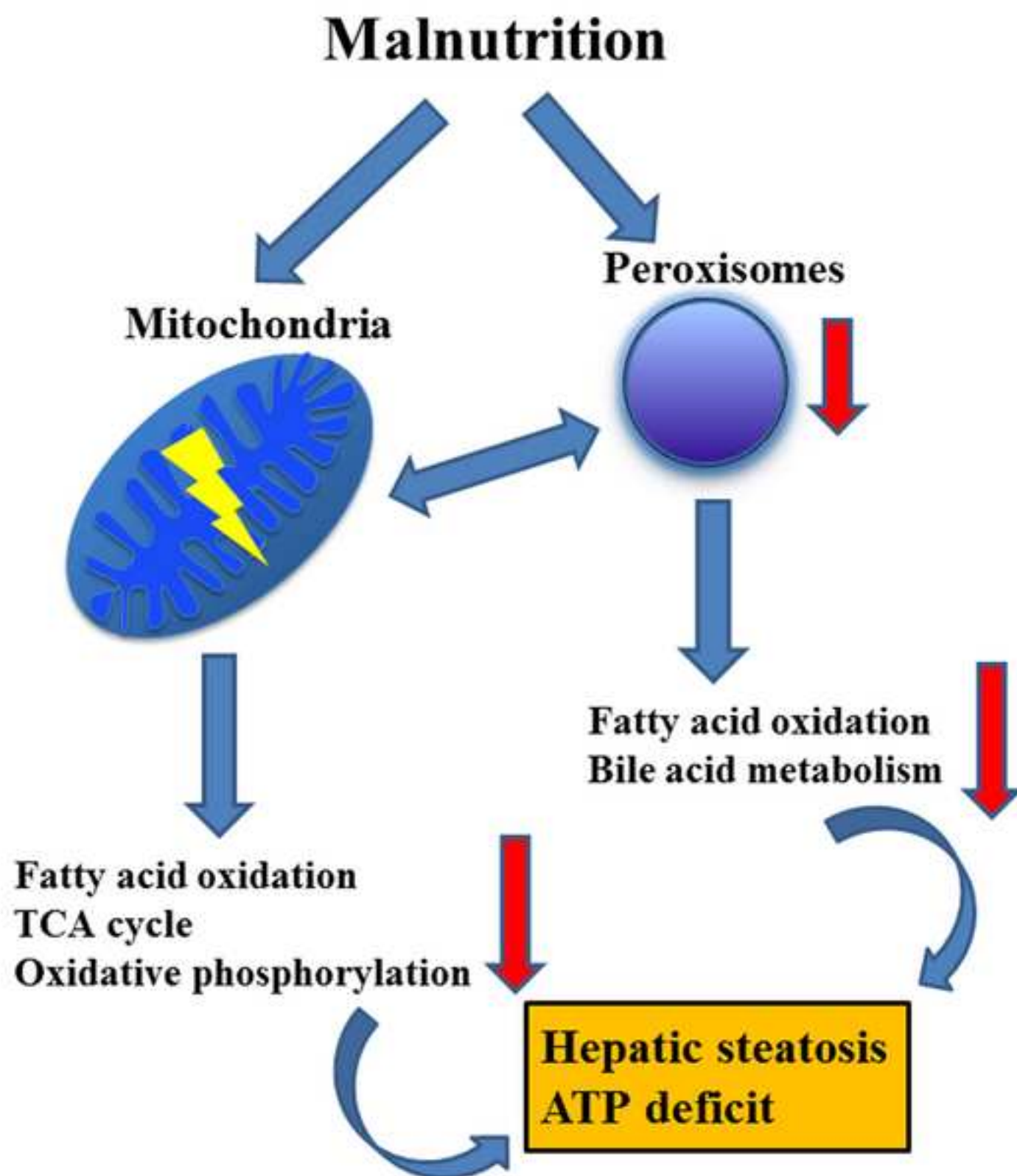












Severe malnutrition in children is associated with metabolic disturbances that are poorly understood. In order to study this further, we developed a malnutrition animal model and found that severe malnutrition leads to an impaired function of liver mitochondria which are essential for energy production and a loss of peroxisomes, which are important for normal liver metabolic function.

ACCEPTED MANUSCRIPT